

Calorimetric Transitions on the Melting Line of the Vortex System as a Function of Oxygen Deficiency in High-Purity $\text{YBa}_2\text{Cu}_3\text{O}_x$

Marlyse Roulin, Alain Junod, Andreas Erb, and Eric Walker

Département de physique de la matière condensée, Université de Genève, 24 quai Ernest-Ansermet, CH-1211 Genève 4, Switzerland

(Received 1 October 1997)

We report adiabatic specific heat measurements for a high-purity $\text{YBa}_2\text{Cu}_3\text{O}_x$ twinned single crystal. The order of the transition on the melting line of the vortex system $B_m(T)$ is investigated for three oxygen concentrations. For $x = 7.00$, no critical end point is observed. For $x = 6.94$, first-order transitions give way to second-order transitions above a tricritical point at a field $B_{cr} = 9.5$ T, and the slope of $B_m(T)$ changes. The latent heat, the slope of $B_m(T)$, and B_{cr} increase with x . Data for less pure crystals are included for comparison purposes. [S0031-9007(97)05280-0]

PACS numbers: 74.25.Bt, 74.60.Ge, 74.62.Dh, 74.72.Bk

The high superconducting critical temperature T_c , the short coherence length ξ , the large anisotropy $\gamma \equiv (m_c/m_{ab})^{1/2}$, and the high upper critical field B_{c2} of high temperature superconductors all contribute to enhance thermal fluctuations. As a consequence, the vortex system melts at temperatures significantly below B_{c2} , a phenomenon that gives rise to anomalies particularly in the magnetoresistance [1], the magnetization M [2,3], and the specific heat C [4–7]. Another consequence is the absence of any abrupt phase transition on the $B_{c2}(T)$ line, which becomes a crossover.

Depending on samples, the vortex melting transition has been reported to be of first or second order. First order means a discontinuity in the first derivatives of the free energy F , i.e., a jump ΔM in the magnetization and a jump ΔS in the entropy (or a δ function in the specific heat). Second order means a discontinuity in the second derivatives of F , i.e., a break in the slope of the magnetization and a jump ΔC in the specific heat. Untwinned crystals of $\text{YBa}_2\text{Cu}_3\text{O}_x$ (YBCO_x) near to optimal doping [4,8] and overdoped twinned crystals of $\text{YBa}_2\text{Cu}_3\text{O}_{7.00}$ [5,6] have shown sharp *peaks* on the melting line $B_m(T)$ which are attributed to first-order transitions between a vortex lattice and a vortex liquid. The latent heat below these peaks is $0.45k_B T$ to $0.6k_B T$ per vortex per CuO_2 layer on the average, in agreement with the observed M jumps [2,3]. Alternatively, the same crystals in fields ≤ 0.5 T [4,8] or ≤ 5 T [5,6], a twinned crystal in fields from 3 to 7 T [9], and a massive but less ordered twinned crystal in fields from 1 to 14 T [5,7] have shown specific heat *steps* practically on the same $B_m(T)$ line. The latter have been attributed to second-order transitions from a vortex glass to a vortex liquid [5,7]. Finally, it has been reported, on the basis of transport measurements, that the first-order transition line may terminate in a critical point near ≈ 10 T on the high field side [10], but calorimetric measurements up to 26.5 T in a fully oxygenated $\text{YBa}_2\text{Cu}_3\text{O}_{7.00}$ crystal have not detected any critical end point [11].

In order to clarify the existence of the critical points on the melting line $B_m(T)$, we have investigated the specific heat of the high-purity crystal of Ref. [6] in oxygen-deficient states. The main experimental result of this study is that the range of fields where specific heat peaks (*first-order transitions*) are observed shrinks and shifts to lower fields, whereas the $B_m(T)$ line is continued by a line of specific heat steps (*second-order transitions*) at both the high- and low-field ends. Therefore the critical end point is closely associated with the presence of oxygen vacancies.

Our calorimetric measurements differ somewhat from the dynamic methods of Refs. [4,8,11] in the sense that they are adiabatic. The resolution is lower, but the experiment yields absolute values. It also requires larger masses, but single crystals with a purity in excess of 99.995% have become available, thanks to the development of nonreactive BaZrO_3 (BZO) crucibles [12]. The crystal under study was grown in BZO, weighs 18 mg, and was previously characterized in its $x = 7.00$ state in Ref. [5,6], to which we refer for experimental details. The new oxygen concentrations studied in the present work were obtained by annealing at various temperatures in 1 bar oxygen and quenching. The values of x are given on the scale of Lindemer [13].

The results are presented in the form of differences $\Delta C(B, T) \equiv C(B, T) - C(0, T)$, i.e., the curve measured in zero field is used as a base line, in order to suppress the large background and to allow the observation of small variations. Note that $C/T \approx 0.10$ to 0.11 J/K² gat in the vicinity of T_c , 1 gat corresponds to ≈ 51.3 g or ≈ 8.0 cm³. The fields are applied at 150 K in order to ensure full penetration. Only data for $B \parallel c$ are discussed here. By repeating some of the experiments, we have verified that small errors in the alignment ($\pm 2^\circ$) do not change the results—in particular, the critical end points. Data for $x = 7.00$ are given in Fig. 1, $x = 6.96$ in Fig. 2, $x = 6.94$ in Fig. 3. Data for $x = 6.92$ were reported in Ref. [6] for a crystal from the same batch; no specific heat peaks were detected.

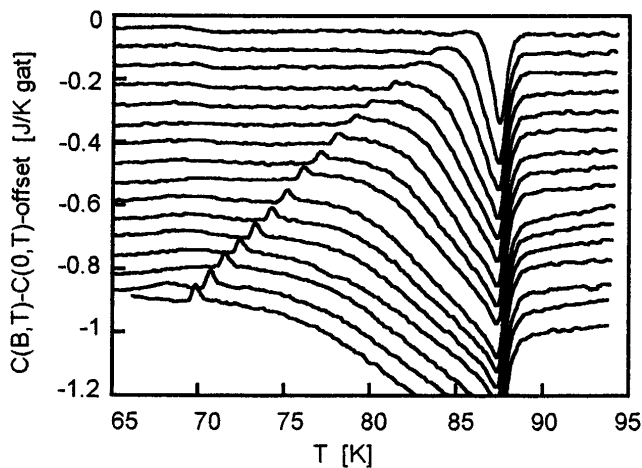


FIG. 1. Difference $C(B, T) - C(0, T)$ versus T for $x = 7.00$. From top to bottom: $B = 1, 2, 3, \dots, 16$ T. The curves are offset for clarity.

The data for the fully oxygenated state (Fig. 1) differ from those of Ref. [4] in several respects. Our ≈ 18 mg crystal is twinned and *overdoped*, i.e., its critical temperature T_c was lowered from the maximum $T_c \approx 93$ K down to $T_c \approx 88$ K by oxidation; at the same time the anisotropy γ was reduced from ≈ 7 to ≈ 5 . This crystal shows specific heat peaks on the melting line only in fields ≥ 6 T, but these peaks are still present in the maximum field of our magnet, 16 T, and at least up to 26.5 T according to the recent experiments of Bouquet *et al.* [11]. The ≈ 3.3 mg crystal studied by Schilling *et al.* is naturally untwinned. Its critical temperature $T_c \approx 92$ K and its anisotropy $\gamma \approx 8$ rather indicate slight underdoping. It shows sharp specific heat peaks from 0.75 to 9 T, the upper limit of measurements. For $B \leq 5$ T in our case, ≤ 0.5 T in Ref. [4], specific heat steps are observed on the continuation of the $B_m(T)$ line.

Figure 2 shows the same crystal as for Fig. 1, this time in the slightly oxygen-deficient state $x = 6.96$. Two dif-

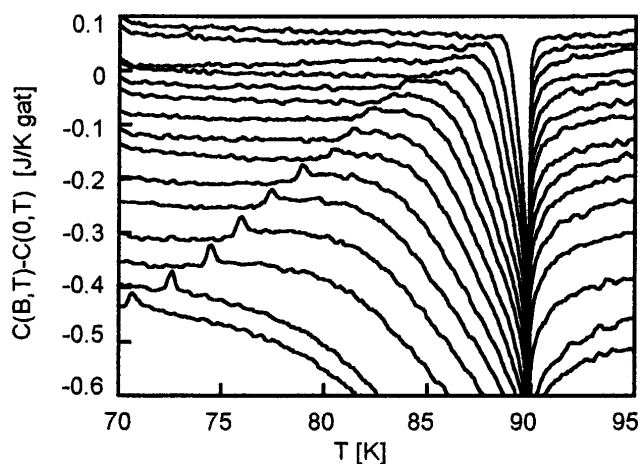


FIG. 2. Difference $C(B, T) - C(0, T)$ versus T for $x = 6.96$. From top to bottom: $B = 0.5, 1, 1.5, 2, 3, 3.75, 4.5, 5.25, 6, 7.5, 9, 10.5, 12, 14,$ and 16 T.

ferences appear with respect to $x = 7.00$: The amplitude of the peaks has decreased (note the different y scale), and the domain where specific heat peaks are seen is slightly more extended at the low-field end ($B \geq 5.25$ T).

Figure 3 shows the same crystal in the state $x = 6.94$; the average undamaged CuO chain length corresponds now to ≈ 17 cells. The low-field limit for the occurrence of specific heat peaks has still decreased ($B \geq 3$ T). The most striking result is the observation of an upper critical point. As shown by the enlargement in Fig. 3(b), the first-order peak is still visible in 9 T; then between 9.5 and 11.5 T it gives way to a specific heat step, and finally for $B \geq 12$ T the curve is smooth on the continuation of the $B_m(T)$ line. Therefore one can define a tricritical point at $B_{cr} \approx 9.5$ T and a critical end point at $B_{end} \approx 11.5$ T for this oxygen concentration.

Figure 4 shows the position of the specific heat anomalies (both peaks and steps) in the B - T phase diagram. The entropy jumps ΔS are obtained by integration of the excess specific heat C/T between a stepped background and the peaks (see Fig. 13 of Ref. [6]). The quantities $\Delta S \Phi_{0s} / k_B B$ in units of k_B per vortex per layer (k_B , Boltzmann's constant; Φ_0 , the flux quantum; and $s = 1.17$ nm, the spacing between CuO₂ bilayers) are given in Fig. 5, which summarizes the general trends: The domain of first-order transitions shifts to lower fields, and the latent heat decreases as the oxygen content is reduced. The width of the peaks does not vary much and remains near 0.5 K, including instrumental broadening.

Generally speaking, a transition between phases with different symmetries (e.g., crystal and liquid) should be

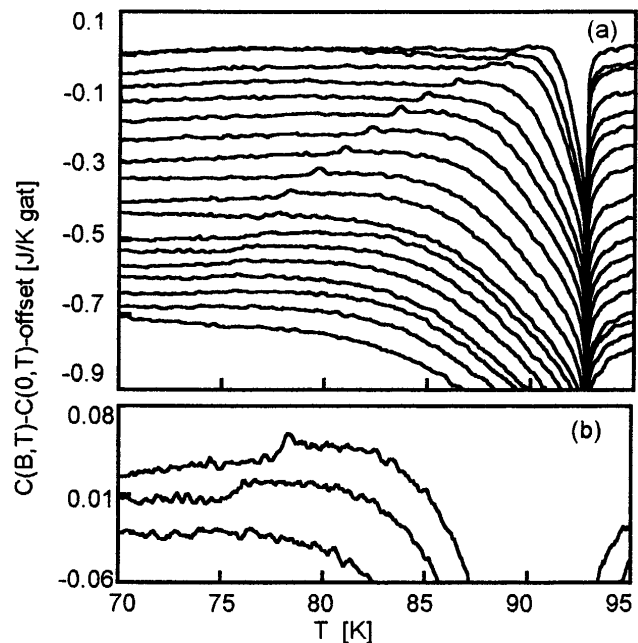


FIG. 3. Difference $C(B, T) - C(0, T)$ versus T for $x = 6.94$. (a) From top to bottom: $B = 1, 1.5, 2, 3, 4, 5, 6, 7, 8, 9, 9.5, 10, 10.5, 11, 11.5, 12, 13,$ and 14 T. (b) $B = 9, 10.5,$ and 13 T. Note the peak near 78 K in 9 T and the step near 76 K in 10.5 T.

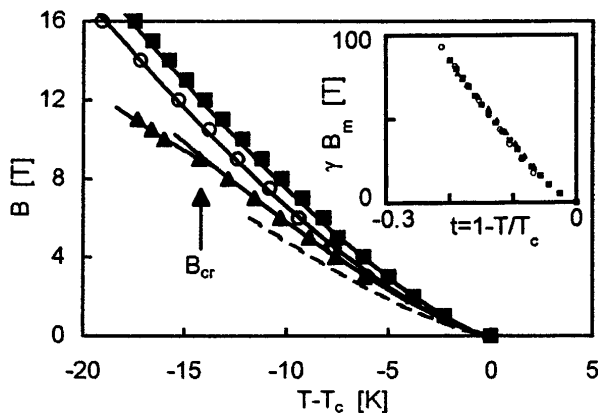


FIG. 4. B - T phase diagram for $x = 7.0$ (■), $x = 6.96$ (○), and $x = 6.94$ (▲). The dashed line is the second-order melting line reported by Roulin *et al.* on (TSFZM)-YBCO_{6.94} [7]. Inset: Product of the melting field by the anisotropy factor, including all values of x .

of first order. In such a case, a critical end point cannot exist. In YBa₂Cu₃O _{x} , we observe both first- and second-order transitions and several critical points. This implies the existence of glass phases; possible phase diagrams are reviewed in Ref. [10].

The observation of a lower tricritical point in YBCO _{x} which separates first-order transitions in $B > B_{\text{low}}$ from second-order transitions in $B < B_{\text{low}}$ is puzzling, especially in view of the 10:1 difference that was reported in the value of B_{low} , depending on samples [4–6]. Although a crossover from first-order to continuous transitions at low fields is indeed predicted by numerical simulations [14], pinning by twin boundaries may also deteriorate the periodicity of the vortex lattice at low fields and result in a Bose glass state; the melting of a Bose glass is expected to be of second order [15]. Detwinning our crystal does not change B_{low} [11], but residual strains could still act as pinning sites. It is interesting that a 2:1 change occurs in B_{low} as a function of the oxygen content (Figs. 1, 3, 5). Noting that twins should vanish for $x \approx 6.3$ when the unit cell becomes tetragonal, it is possible that the decrease of B_{low} reflects a decrease in the twin density on a submicro-

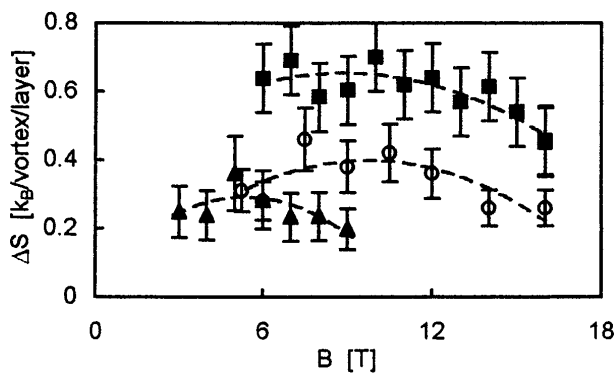


FIG. 5. Entropy jump ΔS per vortex per layer defined by the area below the C/T peak for $x = 7.0$ (■), $x = 6.96$ (○), and $x = 6.94$ (▲). Lines are guides to the eye.

scopic scale (5 T corresponds to a magnetic length scale of 20 nm). However, because we have found that the value of B_{low} is quite reproducible for three fully oxygenated crystals grown in BZO, some intrinsic mechanism cannot be excluded.

The observation of an upper tricritical point separating first-order transitions in $B < B_{\text{cr}} \approx 9.5$ T from second-order transitions in $B > B_{\text{cr}}$ in the underdoped state with $x = 6.94$ confirms by a thermodynamic measurement previous findings based on transport properties [10]. The value of B_{cr} is extremely sensitive to the concentration of oxygen vacancies, and increases to $B_{\text{cr}} > 16$ T for $x = 6.96$. The fact that the upper tricritical point can be shifted to very high values [11] when the oxygen sites are fully occupied shows that its existence is not an intrinsic property of the ideal vortex lattice. Such a point was observed in the related system Bi₂Sr₂CaCu₂O_{8+ x} at a field which also increases with oxygen doping, but which is smaller by 2 orders of magnitude [16]. In the latter case, the tricritical point is followed by a second-order depinning line. We also observe between $B_{\text{cr}} \approx 9.5$ T and $B_{\text{end}} \approx 11.5$ T a line of second-order transitions (C steps). Its slope differs from the main line of first-order transitions (Fig. 4). Because of the nature of our experiments in constant fields, we cannot exclude the existence of a horizontal line of *second peaks* ending in the critical point, such as that reported for Bi₂Sr₂CaCu₂O_{8+ x} [16]. For $B > B_{\text{end}} \approx 11.5$ T, no transition is detected any more. One explanation that has been put forward to explain the absence of first-order transitions in high fields is that because interplanar coupling is weak, the superconductor tends to become 2D, and a 2D system is more susceptible to disorder than a 3D one. In the present case, *disorder* means distribution of oxygen vacancies, or clusters of vacancies [12]. Magnetization cycles measured at $T = 80$ and 70 K show that pinning slowly increases when x decreases (however, no peak of the irreversible magnetization, or *fishtail* anomaly, is observed for $|B| \leq 5$ T and $x \geq 6.94$). This kind of disorder caused by vacancies vanishes for $x = 7.00$. In this sense, the existence of any sort of disorder (defects, impurities, etc.) should also depress the value of B_{end} for $x = 7.00$, so that the very high values found for the present crystal are a measure of its quality.

The shape of the melting lines follows closely a power law $B_m(T, x) = B_{m0}(x)(1 - T/T_c)^n$, $n \approx 4/3$, as long as $B < B_{\text{cr}}$ (Fig. 4 and Table I). The break observed at B_{cr} is consistent with the observations of Safar *et al.* [10]. The melting field B_m and the anisotropy factor γ both decrease when the oxygen concentration x increases. In other words, a trend toward 2D favors melting at lower fields, as illustrated by the very low values for Bi₂Sr₂CaCu₂O_{8+ x} . We find that $B_m(T, x)$ scales experimentally with $1/\gamma$ (Fig. 4, inset). The anisotropy ratio γ was determined by direct comparison of the C/T curves obtained for $B||c$ and for $B||ab$. For example,

TABLE I. Oxygen concentration x , critical temperature T_c (from the inflexion point of the C/T curve at the jump), anisotropy ratio γ , and parameters of the fit of the melting line $B_m(T) = B_{m0}(1 - T/T_c)^n$ for the YBCO $_x$ single crystal.

x	6.94 ± 0.01	6.96 ± 0.01	7.00 ± 0.01
T_c (K)	92.6	89.7	87.8
γ	7.0 ± 0.5	5.9 ± 0.5	5.3 ± 0.5
$B_{m0}(T)$	103	137	135
n	1.3	1.39	1.33

for $x = 6.94$, the curve for $B||c = 1$ T coincides with the curve $B||ab = 7$ T. It follows immediately that $\gamma = 7$.

For $x = 6.96$, our measurements of the latent heat agree with those of Schilling *et al.* [4], but our data show clearly a dependence on the oxygen concentration (Fig. 5).

The specific heat on the freezing line of the vortex system has also been studied recently as a function of the oxygen concentration using massive crystals grown by the traveling solvent floating zone melting technique (TSFZM) [7]. These crystals contain $\approx 5\%$ YBa $_2$ Cu $_2$ O $_5$ by weight, and are less well ordered than BZO crystals. TSFZM crystals show only second-order transitions (C steps) on the melting line. This was recently confirmed independently by small angle neutron diffraction measurements [17], and suggests that the vortex solid is in this case a glass. Because the same oxygen concentrations are available, a comparison is in order. In Fig. 6, we show specific heat curves for (BZO)-YBCO $_{6.94}$ and (TSFZM)-YBCO $_{6.94}$ in a field of 2 T, where both are in the domain of second-order transitions, and in 4 T, where only the purer BZO crystal shows a specific heat peak. It is remarkable that the underlying C step has the same amplitude in both cases, the latter represents the difference between the specific heat of the vortex solid (crystalline or glassy, the difference is small) and that of the liquid. The additional peak in the BZO crystal is related to the loss of translational symmetry upon melting. A second remarkable point is the significant difference in the melting temperatures: The vortex glass melts at a lower temperature than the vortex lattice (Fig. 6). This behavior is systematic, as shown

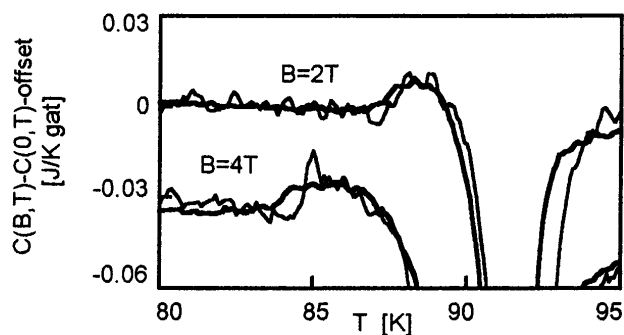


FIG. 6. Difference $C(B, T) - C(0, T)$ versus T for $B = 2$ and 4 T (offset for clarity). Thin lines: (BZO)-YBCO $_{6.94}$. Thick lines: (TSFZM)-YBCO $_{6.94}$ [7].

by the dashed line in Fig. 4, which represents the full second-order melting line of (TSFZM)-YBa $_2$ Cu $_3$ O $_{6.94}$ [7]. A similar situation occurs for crystals which have been disordered by electron irradiation: The melting line is depressed [18], and first-order transitions can be recovered by adequate annealing [19]. The critical end point is also suppressed: $B_{\text{end}} \cong 6$ T for (TSFZM)-YBCO $_{6.94}$ whereas $B_{\text{end}} \cong 11.5$ T for (BZO)-YBCO $_{6.94}$. All these differences are attributed to the higher disorder of the vortex solid in (TSFZM)-YBCO $_x$, which is due to the presence of a relatively large number of randomly distributed pinning sites.

This study of one high-purity YBCO $_x$ crystal at different oxygen concentrations x has shown that oxygen vacancies at high fields, and possibly twins and/or strains at low fields, both contribute to narrow the field range where first-order melting transitions of the vortex lattice can be observed. On both sides of this domain, and over well-defined intervals, melting transitions are still observed, but their second-order nature tends to confirm the existence of the vortex glass state predicted by Fisher *et al.* [20]. The influence of twin boundaries on the lower tricritical point remains to be clarified.

We would like to thank B. Billon, F. Bouquet, C. Marcenat, A. Schilling, N. Phillips, U. Welp, W. K. Kwok, G. W. Crabtree, and J. Muller for fruitful discussions. This research was supported by the Fonds National Suisse de la Recherche Scientifique.

- [1] H. Safar *et al.*, Phys. Rev. Lett. **69**, 824 (1992).
- [2] R. Liang *et al.*, Phys. Rev. Lett. **76**, 835 (1996).
- [3] U. Welp *et al.*, Phys. Rev. Lett. **76**, 4809 (1996).
- [4] A. Schilling *et al.*, Nature (London) **382**, 791 (1996); A. Schilling *et al.*, Phys. Rev. Lett. **78**, 4833 (1997).
- [5] M. Roulin *et al.*, J. Low Temp. Phys. **105**, 1099 (1996).
- [6] A. Junod *et al.*, Physica (Amsterdam) **275C**, 245 (1997).
- [7] M. Roulin *et al.*, Science **273**, 1210 (1996); M. Roulin *et al.*, Physica (Amsterdam) C (to be published).
- [8] B. Billon (private communication).
- [9] A. Schilling *et al.*, in *Proceedings of the 10th Anniversary of HTS Workshop on Physics, Materials and Applications, Houston, Texas, 1996*, edited by B. Battlogg *et al.* (World Scientific, Singapore, 1996), p. 349.
- [10] H. Safer *et al.*, Phys. Rev. Lett. **70**, 3800 (1993).
- [11] F. Bouquet and C. Marcenat (private communication).
- [12] A. Erb *et al.*, Physica (Amsterdam) **245C**, 245 (1995); A. Erb *et al.*, J. Low Temp. Phys. **105**, 1023 (1996).
- [13] T. B. Lindemer *et al.*, J. Am. Ceram. Soc. **72**, 1775 (1989).
- [14] S. Ryu *et al.*, Phys. Rev. Lett. **78**, 4629 (1997).
- [15] D. R. Nelson *et al.*, Phys. Rev. B **48**, 13060 (1993); A. I. Larkin *et al.*, Phys. Rev. Lett. **75**, 4666 (1995).
- [16] E. Zeldov *et al.*, Nature (London) **375**, 373 (1995); B. Khaykovich *et al.*, Phys. Rev. Lett. **76**, 2555 (1996).
- [17] C. M. Aegerter (private communication).
- [18] W. K. Kwok *et al.*, Physica (Amsterdam) **197B**, 579 (1994).
- [19] J. A. Fendrich *et al.*, Phys. Rev. Lett. **74**, 1210 (1995).
- [20] D. S. Fisher *et al.*, Phys. Rev. B **43**, 130 (1991).